

Growth and nonlinear optical properties of GaAs absorber layers for AlGaAs/CaF₂ semiconductor saturable absorber mirrors

S. Schön,^{a)} M. Haiml, M. Achermann, and U. Keller

Institute of Quantum Electronics, Swiss Federal Institute of Technology, ETH-Hönggerberg, HPT, CH-8093 Zurich, Switzerland

(Received 10 October 1999; accepted 31 January 2000)

Absorber layers of semiconductor saturable absorber mirrors are required to show high absorption modulation with recovery times on the order of 100 fs and low nonsaturable losses. While to provide such fast recovery times, defect states for carrier trapping need to be incorporated into the absorber material, defects and surface roughness can cause additional losses in nonsaturable absorption. A specially designed GaAs/fluoride multilayer stack was grown to study the relation between growth conditions, surface roughness, nonsaturable losses, and absorption modulation. The growth of the multilayer stack included three epitaxial growth regimes: (a) homoepitaxial growth of GaAs on GaAs (111) B, (b) heteroepitaxy of CaF₂ on GaAs, and (c) heteroepitaxy of GaAs on CaF₂. While the homoepitaxial and first CaF₂ layer growth proceeded two dimensional, island nucleation was obtained for the GaAs absorber and top CaF₂ layer. The CaF₂ surface was exposed to an electron beam of different doses to increase free surface energy for subsequent GaAs overgrowth and the surface roughness of the absorber layer was found to decrease with increasing electron dose. Nonlinear properties and light scattering were measured and correlated to the growth parameters. Linear reflectivity and absorption modulation were close to the theoretical values of the designed multilayer stack for the region exposed to the highest electron dose. With a recovery time of about 500 fs, the grown GaAs absorber layer is an excellent choice for an all-optical switching application in broadband AlGaAs/CaF₂ semiconductor saturable absorber mirrors. © 2000 American Vacuum Society. [S0734-211X(00)04703-X]

I. INTRODUCTION

Conventional semiconductor saturable absorber mirrors (SESAMs) with their relatively small reflection bandwidth of semiconductor Bragg mirrors are a limiting factor in the wavelength tuning range and the further shortening of pulses from a solid state laser.¹ Al_xGa_{1-x}As/GaAs Bragg mirrors provide a small high reflectance bandwidth of about 60 nm with a large number of mirror pairs (≥ 30). To overcome the refractive index limitation, heteroepitaxy of GaAs/CaF₂ and Al_xGa_{1-x}As/CaF₂ stacks were studied to provide a larger ratio of refractive indices.

For the wavelength range involved (0.5–2 μm), fluorides are nonabsorbing and have no relevant dispersion and low refractive indices, e.g., 1.43 for CaF₂. In contrast, depending on the Al concentration, Al_xGa_{1-x}As ($0 \leq x \leq 1$) have refractive indices larger than 3. Therefore, epitaxially grown GaAs/fluoride Bragg stacks formed a high reflection mirror at 1.4 μm with a 600-nm-high reflection bandwidth and no significant group velocity dispersion.² Al_xGa_{1-x}As/fluoride Bragg mirrors supplied high reflection bandwidth of between 300 and 400 nm at a center wavelength of 780 nm with only four mirror pairs.³

SESAMs can be fabricated by growing spacer and absorber layers on top of broadband Al_xGa_{1-x}As/CaF₂ Bragg mirrors. SESAMs rely on the operation of the absorber layer as an all-optical switch that is based on changes of reflectivity due to absorption bleaching induced by a strong laser

pulse.⁴ The absorber material must show high absorption modulation for recovery times on the order of 100 fs to ps and low nonsaturable losses.

Either low temperature (LT) or ion-implanted GaAs is used as absorber materials for Al_xGa_{1-x}As/GaAs Bragg mirrors. The incorporated As antisites at low growth temperatures or the implanted defects are responsible for carrier trapping causing sub-ps recovery times.^{5,6} While LT growth or ion implantation of GaAs absorber layers for Al_xGa_{1-x}As/GaAs SESAMs is required to create the point defects for fast recovery times, GaAs absorber layers grown on CaF₂ spacer layers on Al_xGa_{1-x}As/CaF₂ Bragg mirrors show extremely fast recovery times due to the high defect concentrations caused by heteroepitaxial growth.

Growth of GaAs on CaF₂ is governed by high lattice mismatches of about 3.5% at room temperature and less than 2.5% at growth temperature and by a large difference in thermal expansion coefficients that causes high thermal strain in the layers during cooling. Furthermore, growth in the (111) orientation was studied to avoid the layer cracking found with the (100) orientation growth and due to strain relaxation in CaF₂. Dislocation gliding relaxes thermal and mismatch strain in (111) oriented layers.⁷ Homoepitaxial growth on (111) oriented GaAs substrates is sensitive to the absolute As pressure, the growth temperature, and the As/Ga flux ratio. Only a small growth window was reported.^{8–11} In addition, the low free surface energy of the CaF₂ surface introduced mainly islanding, stacking faults, rotational twins, or microtwinning in the GaAs growth thereby creating rough

^{a)}Corresponding author; electronic mail: schoen@iqe.phys.ethz.ch

surfaces. Even surfaces mirrorlike to the naked eye can scatter light causing nonsaturable losses and decreasing absorption modulation.

II. EXPERIMENT

The GaAs/CaF₂ stacks were grown in a self-assembled molecular beam epitaxy (MBE) system on GaAs (111)B substrates doped with Si at a concentration of $n_{\text{Si}}=1\times 10^{17}\text{ cm}^{-3}$. Epiready substrates were heated to 300 °C for 12 h before the protective oxide was desorbed under As₂ flux. An effusion cell with Ga trapping-cap system providing As₂ flux, standard Ga, and Al evaporation cells and a water-cooled dual filament cell for CaF₂ were used. Growth temperatures were varied between 570 and 700 °C, and the growth rates were 0.4–0.6 μm/h for GaAs and 0.35–0.8 μm/h for CaF₂. Standard reflection high-energy electron diffraction (RHEED) was used with high voltage varying from 12 to 20 kV. RHEED pattern images shown in this article were observed in the $\langle 110 \rangle$ azimuth. Analysis of the surface was carried out using scanning electron microscopy (SEM) and transmission electron microscopy (TEM). Surface roughness was measured with atomic force microscopy (AFM).

A special design consisting of three layers, namely 90 nm CaF₂, 57 nm GaAs and 148 nm CaF₂, was grown to study the relation between growth conditions, surface roughness, nonsaturable losses, and absorption modulation. Measurements of the pulse energy dependent reflectivity of the multilayer stack were used to determine the absorber's linear reflectivity, R_{lin} , and its changes in reflectivity (modulation depth), ΔR .¹² The temporal decay of the absorption was measured in a standard degenerate time-resolved pump-probe setup. The setup was also used for measurements of scattered light. All measurements were carried out at room temperature using an 80 MHz, 150 fs pulse train from a Ti:sapphire laser centered at 830 nm. The sizes of the laser spots on the sample surface were about 7 and 3 μm in diameter for the nonlinear reflectivity and the pump-probe measurements, respectively.

III. RESULTS AND DISCUSSION

A. Homoepitaxial and heteroepitaxial growth

The growth of the designed layer stack included three epitaxial growth regimes, the homoepitaxial growth of GaAs on GaAs (111) B, the heteroepitaxy of CaF₂ on GaAs and finally the heteroepitaxy of GaAs on CaF₂. A GaAs buffer layer was grown on GaAs (111) B to provide a clean surface for subsequent CaF₂ overgrowth and to find the optimum growth conditions for GaAs absorber growth on CaF₂. Reconstruction patterns of the GaAs (111) B surface revealed sensitive relations between As pressure, Ga flux, and growth temperature. In these studies, homoepitaxial growth of GaAs proceeds three-dimensional (3D) at substrate temperatures $T_s \geq 620$ °C. A variation in the As₂ flux has influence only on the formation of twins; Rotational twins are observed when grown on a (2×2) reconstructed surface and are sup-

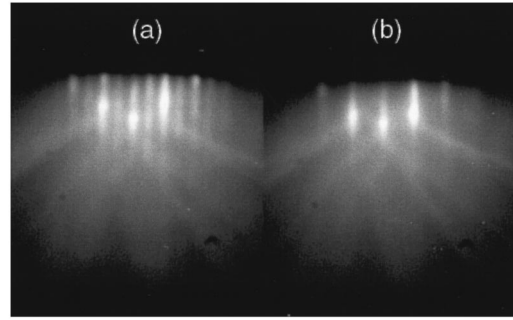


Fig. 1. RHEED pattern images of surface reconstruction taken during growth of the GaAs buffer layer (a) and during growth interruption (b) while As was impinging the surface.

pressed on ($\sqrt{19}\times\sqrt{19}$) reconstructed surfaces, assumed to be Ga rich, by lowering the As flux.¹³ A further decrease in As flux caused permanent disappearance of the surface reconstruction. Two-dimensional (2D) growth was obtained with a growth temperature of 580 °C and by growing 10 Å GaAs with an interruption of 70–100 s while As was impinging on the surface. Starting growth after desorption of the protective oxide, no surface reconstruction was observed up to a thickness of 30 Å, at which time, additional lines appeared in the RHEED pattern indicating first a ($\sqrt{19}\times\sqrt{19}$) surface reconstruction and then a (2×2) surface reconstruction [Fig. 1(a)]. When growth continued, reconstruction lines disappeared [Fig. 1(b)]. While the RHEED pattern was streaky at the beginning, spots on Laue zones developed after 150 Å thickness revealing very good surface quality for subsequent CaF₂ overgrowth. In addition, flat CaF₂/GaAs interfaces were observed in TEM cross section images shown in Fig. 2.

Heteroepitaxial growth of CaF₂ on the GaAs buffer layer was initially carried out at the same growth temperature as the homoepitaxial layer to avoid additional thermal strain caused by a change in substrate temperature. The As₂ beam was turned off for 30 s prior to the CaF₂ growth because too much As on the GaAs surface caused islanding of CaF₂ and resulted in surface roughness. Despite a perfect (2×2) reconstructed GaAs surface, CaF₂ growth did not proceed 2D at a

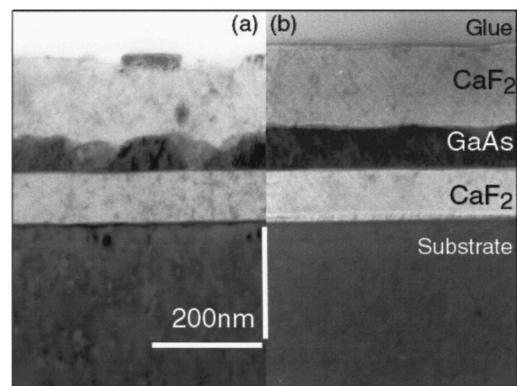


Fig. 2. TEM cross section images of CaF₂/GaAs/CaF₂ on GaAs (111) substrates without (a) and with (b) electron beam modification of the first CaF₂ layer for GaAs overgrowth.

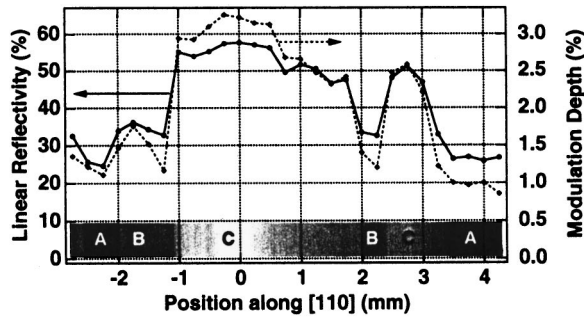


FIG. 3. Linear reflectivity R_{lin} and reflectivity modulation ΔR (right axis) measured vs lateral position on the sample surface. The bar at the bottom is a top view photograph of the corresponding regions A, B, and C of the surface.

growth temperature of 580 °C. A streaky RHEED pattern was observed and rotational twinning was obtained once. However, CaF_2 growth on $(\sqrt{19} \times \sqrt{19})$ reconstructed GaAs surfaces at temperatures $T_s \geq 620$ °C provided spots on zero-order Laue zone in the RHEED pattern indicating a flat CaF_2 surface. Furthermore, while the TEM cross section images of layers grown under these latter conditions (Fig. 2) did not show any misfit dislocations or cracks due to dislocation gliding, a high amount of strain was observed in the layer.

Heteroepitaxy of GaAs on CaF_2 is influenced by the low free surface energy of CaF_2 and a low As sticking coefficient. Furthermore, the (111) orientation is not the preferred growth orientation for GaAs and spontaneous formation of (100) facets during growth has been reported.¹⁴ Growth conditions optimal for the buffer layer growth were applied during the heteroepitaxial overgrowth. Before the Ga flux was allowed to reach the surface, an As flux was applied for between 10 s and 1 min. As has a lower sticking coefficient than Ga and needed to be supplied in excess, but it has been reported that impinging As will form AsF_3 on the F-terminated CaF_2 surface and evaporate from that surface. The As atoms are assumed to form stronger bonds with the Ca atoms and hence modify the free surface energy of the CaF_2 thereby suggesting layer-by-layer nucleation.¹⁵ However, in our studies, GaAs islands nucleated on the CaF_2 surface immediately after Ga had reached the surface. We did not observe any dependence of the growth of the first monolayers on the As impinging time even at higher growth temperatures ($T \leq 620$ °C). We did notice that increasing amounts of As on the CaF_2 surface (≥ 1 min) supported twinning. Since growth on the GaAs islands is energetically preferred to that on the CaF_2 surface, islands grew faster in the vertical direction than in the horizontal. High interface roughness was observed in the TEM cross section image [Fig. 2(a)].

Because surface wetting cannot be improved by impinging As flux, a modification of the CaF_2 surface by an electron beam was studied. It is known that CaF_2 deteriorates when a high energy electron beam hits the surface.¹⁶ Surface regions of the first CaF_2 layer have been exposed to three different electron beam doses while As was impinging on the surface. In the regions A and B shown in the bar of Fig. 3,

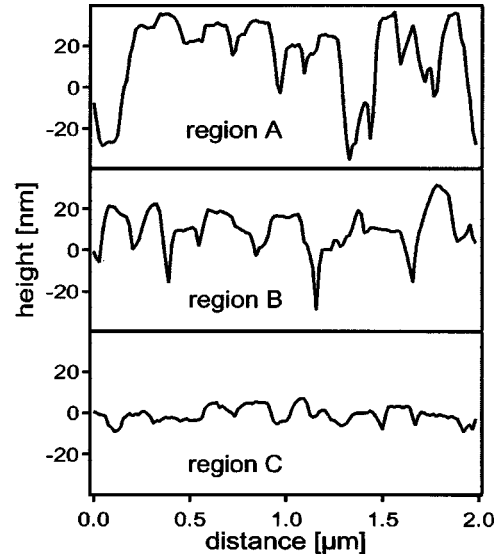


FIG. 4. AFM line scans of surface roughness for regions of different exposed electron doses of 100 (region A), 400 (region B), and 1100 $\mu\text{C}/\text{cm}^2$ (region C).

respective doses of 100 and 400 $\mu\text{C}/\text{cm}^2$ were applied by a focused electron beam before growth. In region C, the CaF_2 surface was exposed to 1100 $\mu\text{C}/\text{cm}^2$ before and during the growth of the first monolayers. Again, the growth conditions of the buffer layer were used. In regime A, no change in the growth and hence no change in the surface morphology in comparison with the unexposed surface was observed. However, regions B and C showed a great improvement in the surface morphology. AFM line scans recorded from the top layer (Fig. 4) showed a decrease in surface roughness with increasing electron dose. The standard deviation of the height profile, a measure to the roughness, was determined to be 16, 12, and 4 nm for the regions A, B, and C, respectively. In addition, the TEM cross section image of region C [Fig. 2(b)] verified much less roughness of the CaF_2/GaAs interface. In all cases, GaAs islands nucleated on the CaF_2 surface. Comparing the TEM images for the unexposed [Fig. 2(a)] and exposed [Fig. 2(b)] region, no change in the layer quality with respect to the defect concentration was observed. The improvement in surface roughness is attributed to an increase in the CaF_2 free surface energy. By breaking the Ca–F bonds with an electron beam, the exposed surface region became more attractive to the GaAs overgrowth. Thus, on the exposed surface the vertical growth is less pronounced than the lateral growth. Hence, less surface roughness appeared in comparison to the growth on the unexposed surface.

The growth of the top CaF_2 layer was more difficult than the growth of the GaAs buffer layer because the absorber layer provided nonflat surfaces, particularly within the unexposed regions. Using the parameters obtained in the growth of the first CaF_2 layer, we noticed that including an annealing step of 10 min or longer after the deposition of 30 Å CaF_2 , helped to flatten the surface. Island growth was always observed. SEM images of the top layer showed trian-

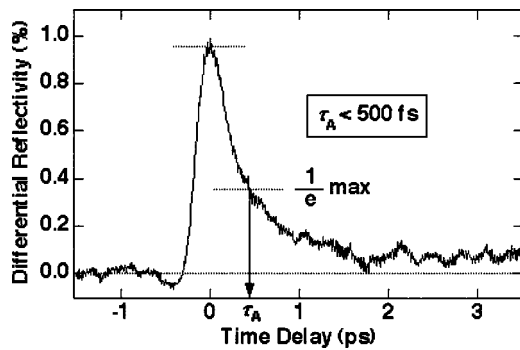


FIG. 5. Differential reflectivity vs time delay between pump and probe pulse. The $1/e$ crossing time is 450 fs.

gularly shaped plateaus with a lateral size up to 200 nm for the exposed regions.

B. Nonlinear optical properties of the absorber layer

The most important parameters of an all-optical switch based on an absorptive nonlinearity are recovery time τ_A , modulation depth ΔR , and nonsaturable absorption losses ΔR_{ns} , as defined by $R_{lin} + \Delta R + \Delta R_{ns} = 1$.¹² In ultrafast semiconductor absorber materials, these parameters are determined by the abundance of selectively incorporated defect states. Unfortunately, defect states can introduce additional nonsaturable absorption and reduce the amount of saturable absorption.¹⁷ Hence, τ_A , R_{lin} , and ΔR reveal information about the crystal quality of the absorber layer.

Poor crystalline quality of the absorber material leads to low modulation depths and high nonsaturable losses, but extremely fast recovery times. The multilayer stack designed for our absorber layer studies has a theoretical value of linear reflectivity of $R_{lin} = 58\%$. Full absorption saturation allowed a modulation depth of $\Delta R = 4.5\%$, while about 40% of the incident light was absorbed by the GaAs substrate. In Fig. 3, the linear reflectivity and the modulation depth of the sample were measured along the $[112]$ orientation covering the above described growth regions, A, B, and C. The value of both parameters varied between the three regions and allowed for identification of the borderlines. No significant changes were seen over a distance of 5 mm along $[110]$ inside region C. For region C, the nonlinear properties were close to the theoretical values of the design with 58% for R_{lin} and up to 3.5% for ΔR , whereas the linear reflectivity in region A dropped to 25%. Here, the modulation depth was proportional to the linear reflectivity and decreased to less than 1%.

A constant recovery time of about 500 fs was observed for all lateral positions, as shown by a representative measurement in Fig. 5. Such a fast recovery time is excellent for the application of the grown GaAs as an absorber material. We can conclude from the constant recovery time measured in all regions, that the intrinsic nonlinear optical properties are the same for all three regions. This result indicates that the number and type of defect, in agreement with our TEM studies, were not dependent on electron exposure.

A mapping of the scattering light with a spatial resolution of less than 10 μm was carried out. The intensity of scattered light normal to the surface from a laser beam incident at 60° to the surface was detected. The amount of scattered light in region A was 30 times higher than in region C. Moreover, the difference between the calculated value for the designed multilayer stack and the amount of scattered light is correlated to the reduction in linear reflectivity. Assuming a spherical distribution and using the value detected for the 0.08 steradian, an extrapolation of light scattered into the half sphere was about 1% in region C and roughly 30%–40% in region A. It can be concluded that the weak nonlinear optical properties in the low dose region were losses due to scattered light. This conclusion is supported by the investigation of the interface morphology and crystalline quality by TEM.

IV. SUMMARY

We have quantitatively investigated the influence of electron assisted growth on the nonlinear optical properties of a GaAs/CaF₂ multilayer stack specially designed for all-optical switching applications in Al_xGa_{1-x}As/CaF₂ SESAMs. The homoepitaxial, (111) oriented GaAs growth and the heteroepitaxial growth of CaF₂ on GaAs and GaAs on CaF₂ were studied. While 2D growth was obtained for buffer layer and first fluoride layer growth, island nucleation was obtained for the absorber layer. Surface and interface roughness was decreased by electron exposure of the fluoride. We found that scattered light caused by surface and interface roughness limited the device performance more than structural defects. With optimum growth conditions, we obtained sub-ps absorber layers with low nonsaturable absorption losses and high absorption modulation. These layers proved to be a good alternative to LT growth and propose the future development of monolithically integrated broadband high-reflecting fluoride mirrors.

ACKNOWLEDGMENT

The authors would like to thank Dr. U. Richter of the Laboratory of Electron Microscopy for the preparation of the TEM cross section images.

- ¹U. Keller, D. A. B. Miller, G. D. Boyd, T. H. Chiu, J. F. Ferguson, and M. T. Asom, *Opt. Lett.* **17**, 505 (1992).
- ²Z. Shi, H. Zogg, P. Müller, I. D. Jung, and U. Keller, *Appl. Phys. Lett.* **69**, 3474 (1996).
- ³S. Schön, H. Zogg, and U. Keller, *J. Cryst. Growth* **201/202**, 1020 (1999).
- ⁴U. Keller, K. J. Weingarten, F. X. Kärtner, D. Kopf, B. Braun, I. D. Jung, R. Fluck, C. Hönninger, N. Matuschek, and J. Aus der Au, *IIEEE J. Sel. Top. Quantum Electron.* **2**, 435 (1996).
- ⁵S. Gupta, M. Y. Frankel, J. A. Valdmanis, J. F. Whitaker, G. A. Mourou, F. W. Smith, and A. R. Calawa, *Appl. Phys. Lett.* **59**, 3276 (1991).
- ⁶M. B. Johnson, T. C. McGill, and N. G. Paulter, *Appl. Phys. Lett.* **54**, 2424 (1989).
- ⁷S. Blunier, H. Zogg, C. Maissen, A. N. Tiwari, R. M. Overney, H. Haefke, P. A. Buffat, and G. Kostorz, *Phys. Rev. Lett.* **68**, 3599 (1992).
- ⁸A. Y. Cho, *J. Appl. Phys.* **41**, 2780 (1970).
- ⁹B. J. Garcia, C. Fontaine, and A. Muñoz-Yagüe, *Appl. Phys. Lett.* **63**, 2691 (1993).
- ¹⁰D. A. Woolf, D. I. Westwood, and R. H. Williams, *Appl. Phys. Lett.* **62**, 1370 (1993).

- ¹¹K. Yang and L. J. Schowalter, *Appl. Phys. Lett.* **60**, 1851 (1992).
- ¹²L. R. Brovelli, U. Keller, and T. H. Chiu, *J. Opt. Soc. Am. B* **12**, 311 (1995).
- ¹³M. Haugk, J. Elsner, M. Sternberg, and T. Frauenheim, *J. Phys.: Condens. Matter* **10**, 4523 (1998).
- ¹⁴K. Young, A. Kahn, S. Horng, and J. M. Phillips, *J. Vac. Sci. Technol. B* **10**, 683 (1992).
- ¹⁵W. Li, T. Anan, and L. J. Schowalter, *Appl. Phys. Lett.* **65**, 595 (1994).
- ¹⁶H. C. Lee, T. Asano, H. Ishiwara, and S. Furukuwa, *Jpn. J. Appl. Phys., Part 1*, **27**, 1616 (1988).
- ¹⁷M. Haiml, U. Siegner, F. Morier-Genoud, U. Keller, M. Luysberg, R. C. Lutz, P. Specht, and E. R. Weber, *Appl. Phys. Lett.* **74**, 3134 (1999).